Arabian Journal of Geosciences (2020) 13:1040
https://doi.org/10.1007/s12517-020-06068-1

ORIGINAL PAPER

Longitudinal study of land surface temperature (LST) using mono- and split-window algorithms and its relationship with NDVI and NDBI over selected metro cities of India

Shahfahad[1] · Babita Kumari[1,2] · Mohammad Tayyab[1,3] · Ishita Afreen Ahmed[1] · Mirza Razi Imam Baig[1] · Mohammad Firoz Khan[1] · Atiqur Rahman[1]

Received: 21 November 2019 / Accepted: 23 September 2020

Abstract

This study was designed to compare the pattern of land surface temperature (LST) over four metro cities of India (Mumbai, Chennai, Delhi, and Kolkata) selected on a longitudinal basis in relation to the built-up and vegetation indices. Two different methods were employed for the retrieval of LST, i.e., mono-window algorithm (MWA) and split-window algorithm (SWA) on the Landsat 8 (OLI/TIRS) datasets, to analyze the spatial pattern of LST over selected cities in relation to normalized differential built-up index (NDBI) and normalized differential vegetation index (NDVI). The result shows that the LST was high over the densely built areas while low over the densely vegetated areas. The highest LST, NDBI, and NDVI were found in Mumbai, while Kolkata records the lowest LST and NDVI. Furthermore, the spatial analysis of LST shows that the LST was high in central parts of all cities except in the case of Delhi where some peripheral areas also record high LST. The comparison from in situ LST (field observations) reveals that the SWA has higher accuracy in the retrieval of LST in maritime areas like Mumbai and Chennai because it reduces the atmospheric effects, while the MWA has higher accuracy for inland areas like Delhi. The spatial relationships of LST with NDVI and NDBI show that vegetation cover has more impact on LST in Delhi while low in Chennai and Mumbai, and the built-up surfaces have a higher impact on LST in Chennai and Mumbai than Kolkata and Delhi.

Keywords Land surface temperature (LST) · Mono- and split-window algorithms · NDVI · NDBI · Longitudinal analysis · Metro cities—India

Introduction

Urbanization is one of the most considerable human activities since the nineteenth century, and about 54% of the world's population was living in urban areas in 2014 (United Nations 2014). During the last three decades, the urban population has rapidly increased in India, which led to a fast expansion of the urban areas (Chettry and Surawar 2020; Mandal et al. 2019). One of the most important changes due to urban expansion is the conversion of natural pervious land surfaces into artificial built-up surfaces (Lu et al. 2008). This reduces the surface albedo and significantly changes thermal conductivity and

Responsible Editor: Biswajeet Pradhan

✉ Atiqur Rahman
ateeqgeog@yahoo.co.in

Shahfahad
fahadshah921@gmail.com

Babita Kumari
pihu.mital@gmail.com

Mohammad Tayyab
tayyab617@gmail.com

Ishita Afreen Ahmed
ishita182382@st.jmi.ac.in

Mirza Razi Imam Baig
mrib786@gmail.com

Mohammad Firoz Khan
mohdfirozkh@gmail.com

[1] Department of Geography, Faculty of Natural Sciences, Jamia Millia Islamia, New Delhi 110025, India

[2] The INCLEN Trust International, Okhla Industrial Area Phase - 1, New Delhi, India

[3] Delhi Development Authority (DDA), New Delhi, India

heat capacity of the surface, thus more heat gets stored in the urban surfaces (Wonorahardjo et al. 2020; Omidvar et al. 2019; Mohajerani et al. 2017), which leads to increasing the land surface temperature (LST) in urban areas (Wonorahardjo et al. 2020; Li et al. 2020). The land surfaces experience a complex alteration in the process of urbanization in which the naturally vegetated areas are mostly transformed into the impervious surfaces (Sharpe et al. 1986). The vegetation growth is generally slow in the urban areas, and it is high in the suburbs than the city center (Takagi and Gyokusen 2004).

The urban built-up area increases at the cost of natural surfaces such as agricultural land, natural vegetation, and water bodies (Pramanik and Punia 2019; Rahman et al. 2011). This leads to changes in thermal properties of the surfaces, and thus, more heat gets stored in the land surfaces (Li et al. 2018; Lu et al. 2008). The changing thermal properties of the land surface due to urban expansion lead to the increasing LST and development of urban heat island (UHI) phenomenon in urban areas (Munslow and O'Dempsey 2010). The natural pervious and artificial surfaces have significant differences in LST (Connors et al. 2013) because of the differences in the thermal properties of the surfaces.

The built-up surfaces always have higher LST than the vegetation cover because of low surface reflectance and more heat capacity, which makes cities warmer than their surrounding countryside (Yang et al. 2017; Su et al. 2010). The difference in LST of rural and urban areas shows that the urbanization has a significant impact on LST (Bian et al. 2017). The green patches in urban areas mitigate the near-surface and surface temperature that results in low LST, but the magnitude of mitigation effect depends on the type and composition of vegetation (Asgarian et al. 2014). The LST of any area depends on the biophysical conditions, neighborhood environment (Mujabar and Rao 2018), climatic conditions, and type and composition of the land use pattern (Zhang et al. 2016), and is due to population growth (Mallick and Rahman 2012) and due to variations in elevation (Khandelwal et al. 2018). The LST in urban areas is influenced and controlled by several factors, and the highest LST is also found outside the city over barren surfaces (Aldhshan and Shafri 2019), because the urban surfaces absorb and release the temperature slowly than the barren land, hence barren land also exhibit higher LST (Ibrahim 2017). The changes in surface heat fluxes due to anthropogenic aerosols, solar radiation, changes in land surface composition, etc. also influence the LST (Sahana et al. 2019).

The various processes of the earth system like physical, chemical, and biological play dominating role in controlling the LST, whereas thermal satellite imageries are proven to be an important tool to assess and monitor land use pattern and LST at the different spatial and temporal resolutions, because there is no other source to get such detailed information on LST (Becker and Li 1990). Due to the advancement in satellite remote sensing, the mapping and monitoring of urban growth and its impacts have become possible at various scales (Khadim et al. 2016; Xie et al. 2008). Studies have been carried out on index-based assessment of urban built-up surface and vegetation cover and their relationships with LST (Guha et al. 2018; Deng et al. 2017; Ogashawara and Bastos 2012; Chen et al. 2006). The LST has a positive relationship with normalized differential built-up indices (NDBI), while a negative relationship with normalized differential vegetation indices (NDVI), i.e., the higher the NDBI, the higher will be the LST, and the lower the NDBI, the lower will be the LST, and vice versa (Kumari et al. 2018; Mwangi et al. 2018). The NDVI has a negative relationship with LST because of the evapotranspiration effect where heat gets transferred back to the atmosphere in one form or another (Voogt and Oke 2003), whereas the NDBI has a positive relationship with LST because the emissivity of the built surface is low and thus heat gets stored for a longer time (Xiao and Weng 2007).

Guo et al. (2012) produced an urbanization index to find the relationship between urbanization and LST, which shows that the urbanization has a complicated but strong and positive relationship with LST. Urban density, i.e., density of impervious surfaces is one of the indicators of the urbanization index, also has a strong positive relationship with LST (Bonafoni and Keeratikasikorn 2018). Ogashawara and Bastos (2012) studied the relationship of built-up area, water bodies, and vegetation density with the LST and pointed out that the built-up surfaces have significantly high LST while the presence of vegetation cover and water bodies reduces the LST. The NDBI is more effective in describing LST than NDVI during any time of the year because the NDVI varies with seasons but the NDBI did not change with seasons and remains the same throughout the year (Guha et al. 2018; Chen et al. 2006). The LST is influenced by three factors: energy transformation of cities, evapotranspiration variation, and increase in the emission of energy from anthropogenic sources (Wang et al. 2020; Lombardo 1985). Furthermore, the retrieval of LST from satellite data uses the data from three variables (atmospheric, angular, and emissivity) beside satellite data (Franca and Cracknell 1994). All the previous studies on LST in India have used single algorithm for the LST retrieval: either radiance method, mono-window algorithm (MWA), split-window algorithm (SWA), or single-channel method by using one of the three variables mentioned above (Dutta et al. 2019; Sahana et al. 2019; Patra et al. 2018; Mallick et al. 2013). Therefore, in this study, two methods for LST retrieval were employed, i.e., split-window algorithm (SWA) and mono-window algorithm (MWA), by using two of the three variables, i.e., surface emissivity and atmospheric effect.

Studies have been done to analyze the LST and its relationship with vegetation cover and the built-up area of Mumbai (Dwivedi and Khire 2018; Sahana et al. 2019), Chennai (Amirtham et al. 2009), Kolkata (Ghosh et al. 2019; Aithal et al. 2019), and Delhi (Dutta et al. 2019; Mallick et al. 2013; Mallick and Rahman 2012). All these previous studies were

done in isolation for either one or two cities. Studies have been done to compare the variation of LST over different mega-cities of China (Liu et al. 2020), Italy (Guha et al. 2018), South-East Asia (Masoudi et al. 2019), USA (Fu and Weng 2018), etc., but there is a lack of this kind of studies in India. Although some studies were done to analyze the spatial and temporal pattern of LST and its relationships with the land use/land cover (LU/LC) changes for selected Indian cities during the recent past (Aithal et al. 2019; Sultana and Satyanarayana 2018; Grover and Singh 2015), none of the studies has compared the LST pattern and its differences over the largest metropolitan cities of India. Therefore, the main objective of this study was to compare the relationship of NDVI and NDBI with LST over the four largest metro cities of India selected on the longitudinal basis starting from Mumbai, Delhi, Chennai, and Kolkata. The cities selected for this study are the top four largest cities in terms of urbanization and economic growth, etc. Another objective was to compare the LST retrieved using two different methods, i.e., MWA and SWA, over the selected cities.

Study area

The four largest metro cities of India located on different longitudes (Fig. 1) were selected for the comparative analysis in the present study. According to the Census of India (2011), these four cities are the home of more than 32 million population, Mumbai being the largest followed by Delhi, Chennai, and Kolkata (Table 1). Due to their large size, high population concentration, and high urban density, these cities are witnessing significant changes in climatic condition and experiencing extreme climatic events in terms of heat waves, extreme precipitation, smog, etc.

These cities vary not only in terms of size and population but also in terms of climatic conditions. Mumbai has a hot and moist climate, and it receives maximum precipitation from south-west monsoon from July to September with an average annual temperature of 27.2 °C (Sahana et al. 2019). Delhi has a semi-arid type climate having an average annual temperature about 25.1 °C and receives most of its precipitation from south-east monsoon from July to September (Dhorde et al. 2009). Chennai is located in the southern part of India and has a hot and moist type of climate with an average annual temperature of 28.6 °C and receives most of its rainfall during October to December from retreating monsoon (Dhorde et al. 2009). Kolkata has a moderate climate with an average annual temperature of 24.8 °C. It receives maximum rainfall during June and September but pre-monsoon showers start from March, which is known as Norwester (Sadhukhan et al. 2000). Among all cities, Delhi has a continental location, thus it has maximum variation in weather while the rest of the cities have less weather variation due to the maritime effect.

Database and methodology

Database

The satellite data used in this study were downloaded from the US Geological Survey (USGS) website https://earthexplorer.usgs.gov/. Landsat 8 (OLI/TIRS) red, near-infrared, and middle infrared bands (bands 4, 5, and 6) have been used for calculation of NDVI and NDBI, while thermal bands (bands 10 and 11) were used for retrieval of LST for March 2017 (Table 2). Maps of the cities are taken from the Survey of India (SOI) toposheet at a scale of 1:25000.

Methodology

We select four cities of India, Chennai, Delhi, Kolkata, and Mumbai, for this study to assess the spatial pattern of LST using two different algorithms, i.e., MWA and SWA. The MWA uses a single band, i.e., band 10, and provides better accuracy in LST than the average of band 10 and band 11 (Sekertekin and Bonafoni 2020). The SWA uses both thermal bands to calculate the LST and considers atmospheric water vapor content, thus it removes the atmospheric effects (Wan and Dozier 1996). The use of SWA is important in the case of coastal areas because weather effects are maximum on satellite-derived LST in these areas. The area of interest (AOI) of the boundary of the cities was extracted from the SOI toposheet using ArcMap 10.2. The NDVI and NDBI were calculated for these cities using Landsat data in the ERDAS Imagine software version 14. Furthermore, the spatial

Table 1 Description of the size and location of cities

S. No.	Cities	Area (km²)	Population (in millions)	Latitude	Longitude
1	Mumbai	603.4	12.40	18° 58′ 30″ N	72° 49′ 33″ E
2	Delhi	1484	11.03	28° 36′ 36″ N	77° 13′ 48″ E
3	Chennai	426	4.64	13° 08′ 27″ N	80° 27′ 07″ E
4	Kolkata	205	4.49	22° 57′ 26″ N	88° 38′ 39″ E

Source: Census of India 2011

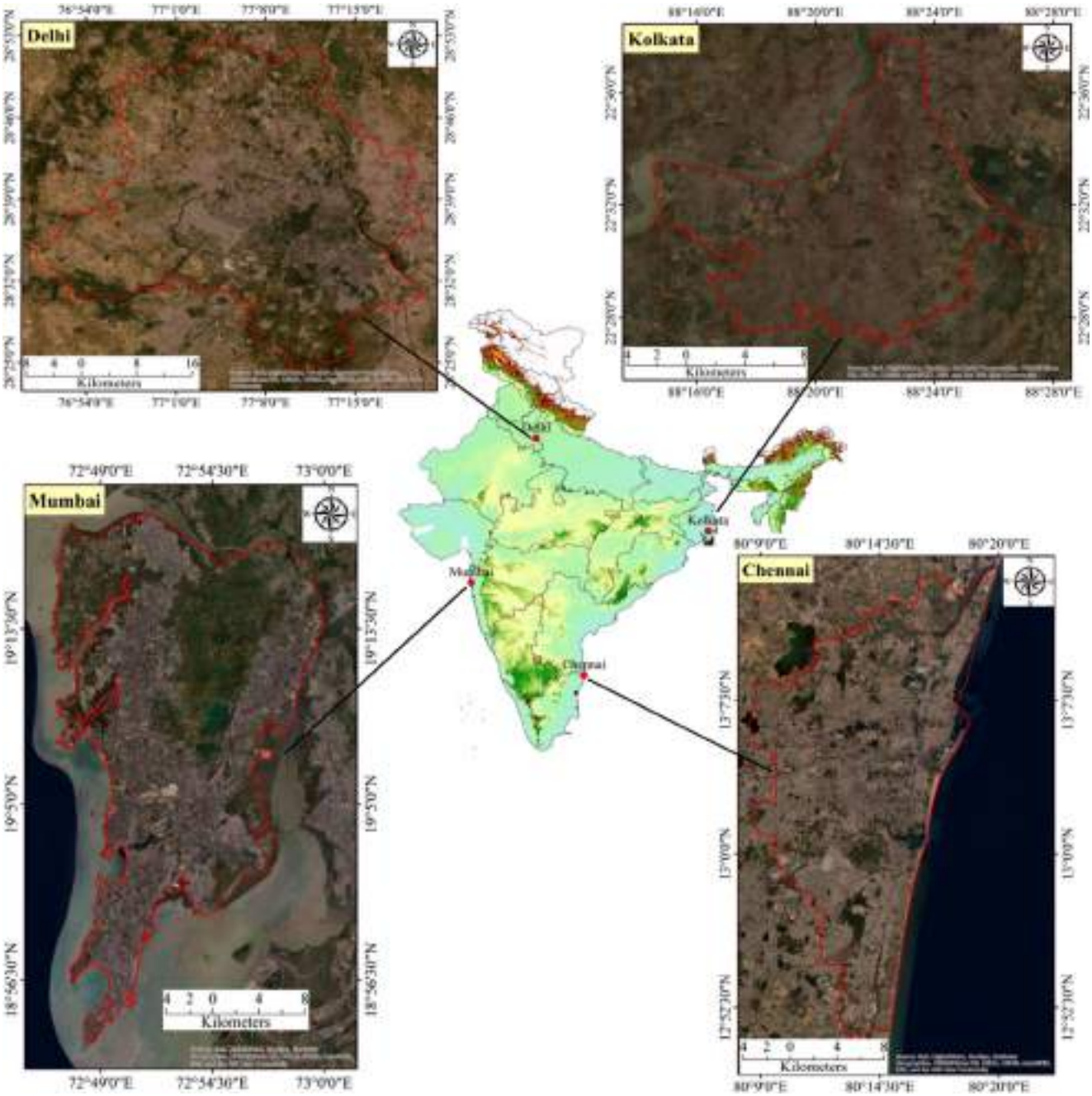

Fig. 1 Location of the study areas

relationship between LST and NDVI has been analyzed using simple linear regression.

Calculation of normalized differential vegetation index

The NDVI is the most widely and most popular tool for assessing the vegetation distribution and density in any part of the world. The NDVI was calculated using red and near-infrared bands because these bands have the highest absorption of electromagnetic energy by chlorophyll (Xue and Su 2017). It is an indicator of surface emissivity and surface energy balance, thus it has impacts on LST (Lo et al. 1997). The NDVI was calculated using Eq. 1.

$$\mathrm{NDVI} = \frac{\mathrm{NIR}-\mathrm{Red}}{\mathrm{NIR}+\mathrm{Red}} \tag{1}$$

Table 2 Details of the satellite data used

S. No.	Cities	Satellite	Bands	Acquisition date	Path/row	Spatial resolution
1	Chennai	Landsat 8 (OLI/TIRS)	4, 5, and 6	25 March 2017	142/51	30 m
			10 and 11			100 m
2	Delhi	Landsat 8 (OLI/TIRS)	4, 5, and 6	21 March 2017	146/40	30 m
			10 and 11			100 m
3	Kolkata	Landsat 8 (OLI/TIRS)	4, 5, and 6	13 March 2017	138/44	30 m
			10 and 11			100 m
4	Mumbai	Landsat 8 (OLI/TIRS)	4, 5, and 6	19 March 2017	148/47	30 m
			10 and 11			100 m

Calculation of normalized differential built-up index

The calculation of the NDBI was done to map the impervious surfaces, using near-infrared and short-wave infrared bands using Eq. 2, proposed by Zha et al. (2003). For Landsat 8, band 5 is near-infrared and band 6 is short-wave infrared bands.

$$\mathrm{NDBI} = \frac{\mathrm{SWIR}-\mathrm{NIR}}{\mathrm{SWIR}+\mathrm{NIR}} \tag{2}$$

Retrieval of LST using mono-window algorithm

The retrieval of LST using the MWA involves the calculation of brightness temperature, calculation of the proportion of vegetation, and emissivity correction (Fan et al. 2017). In the first step, the brightness temperature was derived from the top-of-atmosphere (TOA) reflectance with the help of calibration constants given in metadata (Chander et al. 2009). In the next step, the NDVI threshold method (Sobrino et al. 2004) was applied for emissivity correction. The NDVI method considers a pixel as bare soil if NDVI is less than 0.2, sparse vegetation if NDVI is between 0.2 and 0.5, and dense vegetation if NDVI is above 0.5 (Fan et al. 2017). The proportion of vegetation (Pv) was calculated using Eq. 3 given by Carlson and Ripley (1997).

$$Pv = \left[\frac{\mathrm{NDVI}-\mathrm{NDVImin}}{\mathrm{NDVImax}-\mathrm{NDVImin}}\right]^2 \tag{3}$$

In the next step, the emissivity correction was done using a modified coefficient of emissivity retrieval of Yu et al. (2014) given in Eq. 4.

$$\varepsilon = 0.00149Pv + 0.98481 \tag{4}$$

where ε is the surface emissivity and Pv is the proportion of vegetation calculated in Eq. 2. In the next step, the LST was calculated using Eq. 5 proposed by Artis and Carnahan (1982).

$$T = \frac{TB}{1 + (\lambda \cdot TB/P)ln(\varepsilon)} \tag{5}$$

where, T is the LST in Kelvin; TB is the brightness temperature derived from the top of atmosphere; λ is the wavelength of emitted radiance (i.e., 10.8 μm for Landsat 8), $P = h \times c/s$ (1.4388×10^{-2} m K), where h is Planck's constant (6.624×10^{-34}J s), c is the velocity of light (2.998×10^{8} m/s), and s is the Boltzmann constant (1.38×10^{-23} J/K); and ε is the surface emissivity. In the final step, the LST was converted into Celsius using Eq. 6.

$$T(°\mathrm{C}) = T - 273.15 \tag{6}$$

where T (°C) is the temperature in Celsius, T is the LST calculated in Kelvin, and 273.15 is the constant.

Retrieval of LST using split-window algorithm

The estimation of LST using the SWA proposed by McMillin (1975) involves the calculation of brightness temperature at the top of atmosphere, estimation of land surface emissivity (LSE), and estimation of atmospheric water vapor content. In the first step, the brightness temperature was derived from the TOA reflectance for bands 10 and 11. In the next step, the fraction of vegetation cover (FVC) was calculated using Eq. 7.

$$\mathrm{FVC} = \frac{\mathrm{NDVI}-\mathrm{NDVIsoil}}{\mathrm{NDVIveg.}-\mathrm{NDVIsoil}} \tag{7}$$

The estimation of LSE requires the emissivity of vegetation as well as soil for both thermal bands (Table 3). The LSE is

Table 3 Emissivity values based on Skokovic et al. (2014)

S. No.	Emissivity	Band 10	Band 11
1	Vegetation (εv)	0.971	0.977
2	Soil (εs)	0.987	0.989

calculated for both thermal bands individually as given in Eq. 8. In the next step, the mean LSE (m) and LSE difference (Δm) were calculated by combining the LSE of band 10 and band 11.

$$\mathrm{LSE} = \varepsilon s \times (1-\mathrm{FVC}) + \varepsilon v \times \mathrm{FVC} \quad (8)$$

In the next step, the atmospheric water vapor content (w) was calculated using Eq. 9 derived from ideal gas Eq. 9.

$$w = \frac{0.622 \times Pv}{P-Pg} \quad (9)$$

where Pv is the compound of relative humidity (RH) and saturation vapor pressure (Pg), P is the total atmospheric pressure, and 0.622 is the constant. The calculated atmospheric water vapor content (w) of all cities is given in Table 4.

Finally, the LST was calculated using split-window coefficient values ($C0$–$C6$) given in Table 5, atmospheric water vapor content, and LSE (Eq. 10)

$$\begin{aligned}\mathrm{LST} = {} & TB10 + C1 \times (TB10-TB11) + C2 \\ & \times (TB10-TB11)2 + C0 + (C3 + C4w) \\ & \times (1-m) + (C5 + C6w) \times \Delta m \end{aligned} \quad (10)$$

where, $TB10$ and $TB11$ are brightness temperature at the TOA, C_1–C_6 are split-window coefficients given in Table 5, m is the mean LSE, Δm is the LSE difference, and w is the atmospheric water vapor content. In the last step, the LST was converted from Kelvin to Celsius using Eq. 6.

Comparison between observed (in situ) and estimated LST and LSE

Two different methods for the validation of LST were identified, i.e., ground measurement and the near-surface air temperature (Li et al. 2013). While the former has an error from 2–5 °C, in the case of the latter, it can have higher differences (Rangoli et al. 2018). Thus, ground-based measurement using a handheld infrared thermometer (over the same geo-coordinate position) was used to validate the estimated LST. The numbers of measurements were taken proportionally in relation to the area of the city. Firstly, the estimated temperatures were reclassified into 4 sub-classes (low-, medium-, high-, and very high–temperature classes), and then, the ground measurements were taken in such a way that it covers all the four temperature classes. Consequently, 50, 75, 150, and 325 measurements were taken for Kolkata, Chennai, Mumbai, and Delhi, respectively. The location of the ground measurement site also depends on the accessibility to reach the site and perform the ground measurement. Thus, measurements were not taken from the inaccessible dense forests, water bodies, and mangrove forests of coastal cities (Chennai, Kolkata, and Mumbai).

The estimated LST was from March 2017, but the ground (in situ) measurements were taken in the afternoon of the cloud-free days (after 01:30 PM) during the second, third, and fourth week of March 2018 because the ground observations for March 2017 were not available. The result shows that the in situ LST is lower than the LST-SWA but higher than the LST-MWA in all the cities. However, the difference between in situ LST and LST-MWA was lower in Delhi and between in situ LST and LST-SWA was comparatively higher in Delhi among all the cities. The difference between ground measurement and LST-MWA ranges between 0.36 and 2.1 °C, 0.31 and 2.34 °C, 0.68 and 3.27 °C, and 0.73 and 3.43 °C for Delhi, Kolkata, Chennai, and Mumbai, respectively. On the other hand, the difference between ground measurement and LST-SWA ranges between 1.48 and 7.62 °C, 0.73 and 4.32, 2.39 and 6.59, and 2.42 and 6.97 for Delhi, Kolkata, Chennai, and Mumbai. The Pearson correlation technique has been used to analyze the trend of estimated measurements of LST and surface emissivity in relation to the ground measurement. The correlation coefficient shows strong positive relationships between the estimated and in situ measurements (Table 6).

Statistical analysis

For statistical analysis, firstly, the raster imageries were converted into point–pixels using the conversion tool in the ArcGIS 10.2 domain, and then the pixel values of each file were transferred into MS Excel format. The LST calculated using MWA was used for statistical analysis because the error was found less for MWA than SWA. In the next step, the pixels were randomly selected from each part of the city in

Table 4 Calculated atmospheric water vapor content (w) of the Indian cities

S. No.	City	w
1	Chennai	0.045
2	Delhi	0.035
3	Kolkata	0.042
4	Mumbai	0.036

Table 5 Split-window coefficients

S. No.	Constant	Value
1	$C0$	− 0.268
2	$C1$	1.378
3	$C2$	0.183
4	$C3$	54.300
5	$C4$	− 2.238
6	$C5$	− 129.200
7	$C6$	16.400

Table 6 Correlation between in situ and estimated measurements

S. No.	City	Correlation between estimated and in situ measurement		
		LST-MWA	LST-SWA	Emissivity
1	Mumbai	0.81	0.84	0.79
2	Delhi	0.82	0.79	0.77
3	Chennai	0.81	0.83	0.78
4	Kolkata	0.78	0.81	0.76

the proportion of the area of the city for statistical analysis. Thus, 300, 600, 250, and 200 pixels were selected for Mumbai, Delhi, Chennai, and Kolkata respectively, and the simple linear regression technique was applied on the selected pixel values in MS Excel to calculate the spatial relationships between LST and NDBI and LST and NDVI.

Results

Analysis of NDVI and NDBI

The NDVI is an indicator of the distribution and health of vegetation in an area at any time of observation, while the NDBI is an indicator of the built-up area of an area. Both NDVI and NDBI values range between − 1 and + 1 (Malik et al. 2019), in which the negative value reflects the absence of vegetation or built-up area and the positive values reflect the presence of vegetation or built-up area for both indices respectively. The lower value reflects scattered vegetation or built-up area for NDVI and NDBI, and the higher values reflect denser vegetation or built-up area respectively (Sobrino et al. 2004).

Analysis of statistical values of NDVI and NDBI

The result of the study shows that the NDVI or vegetation greenness was maximum and well pronounced in Mumbai and Delhi and low and less prominent in the Chennai and Kolkata, although the maximum NDVI value was in Chennai. But the NDBI or built-up density was almost similar in all the four cities although Mumbai and Delhi have a few more patches of the highly dense built-up area than others (Fig. 2). The descriptive statistics show that the highest value of both maximum and minimum NDVI was in Chennai followed by Mumbai and Delhi, while Kolkata is on the bottom of the table with the least maximum NDVI value which connotes that the former two cities have maximum variation in vegetation while the latter have low variation (Table 7). Furthermore, the highest value of the maximum and minimum NDBI was found in Mumbai and Delhi, while Chennai has the lowest maximum NDBI value (Table 7).

Furthermore, in terms of mean values, Delhi has the highest mean for both NDVI and NDBI, while Mumbai and Chennai stand second for mean NDVI and NDBI, respectively. This shows that Delhi has the highest cover of both vegetation cover as well as the built-up area. On the other hand, Kolkata has the least mean NDVI and NDBI, showing that the city has the least high built-up as well as vegetation cover among all the selected cities. The standard deviation of NDVI and NDBI was maximum in Delhi followed by Mumbai, while Chennai and Kolkata have the same standard deviation of NDVI and NDBI (Table 7), which means that the distribution of NDVI and NDBI both has more variation in Delhi and Mumbai in comparison with Chennai and Kolkata.

Analysis of spatial pattern of NDVI and NDBI

The NDVI and NDBI values of Mumbai range between − 0.22 and 0.54 and − 0.48 and 0.45 respectively. The green cover was more pronounced in Mumbai than other cities and was maximum in the northern parts of the city. It extends along the bays and in a long belt of high NDVI value from the central part to the northern extreme of the city. The small patches of high NDVI value occur in the eastern as well as the western part along the bay area, while the NDVI value was lowest over the Virar, Powai, and Tulsi lakes in the central part as well as in the small water bodies located at the northern extreme, although it was also low in central, northern, and southern parts of the city (Fig. 2a). On the other hand, the NDBI value was the highest in the south-central part as well as at the southern tip of the city and in northern parts above the

Table 7 Descriptive statistics of NDVI, NDBI, and NDMI for all cities

Cities	NDVI				NDBI			
	Min.	Max.	Mean	SD	Min.	Max.	Mean	SD
Mumbai	− 0.22	0.53	0.15	0.08	− 0.48	0.45	− 0.05	0.07
Delhi	− 0.08	0.51	0.16	0.09	− 0.26	0.42	0.08	0.08
Chennai	− 0.12	0.57	0.14	0.07	− 0.39	0.38	− 0.02	0.06
Kolkata	− 0.08	0.48	0.14	0.07	− 0.35	0.42	− 0.06	0.06

Min., minimum; *Max.*, maximum; *SD*, standard deviation

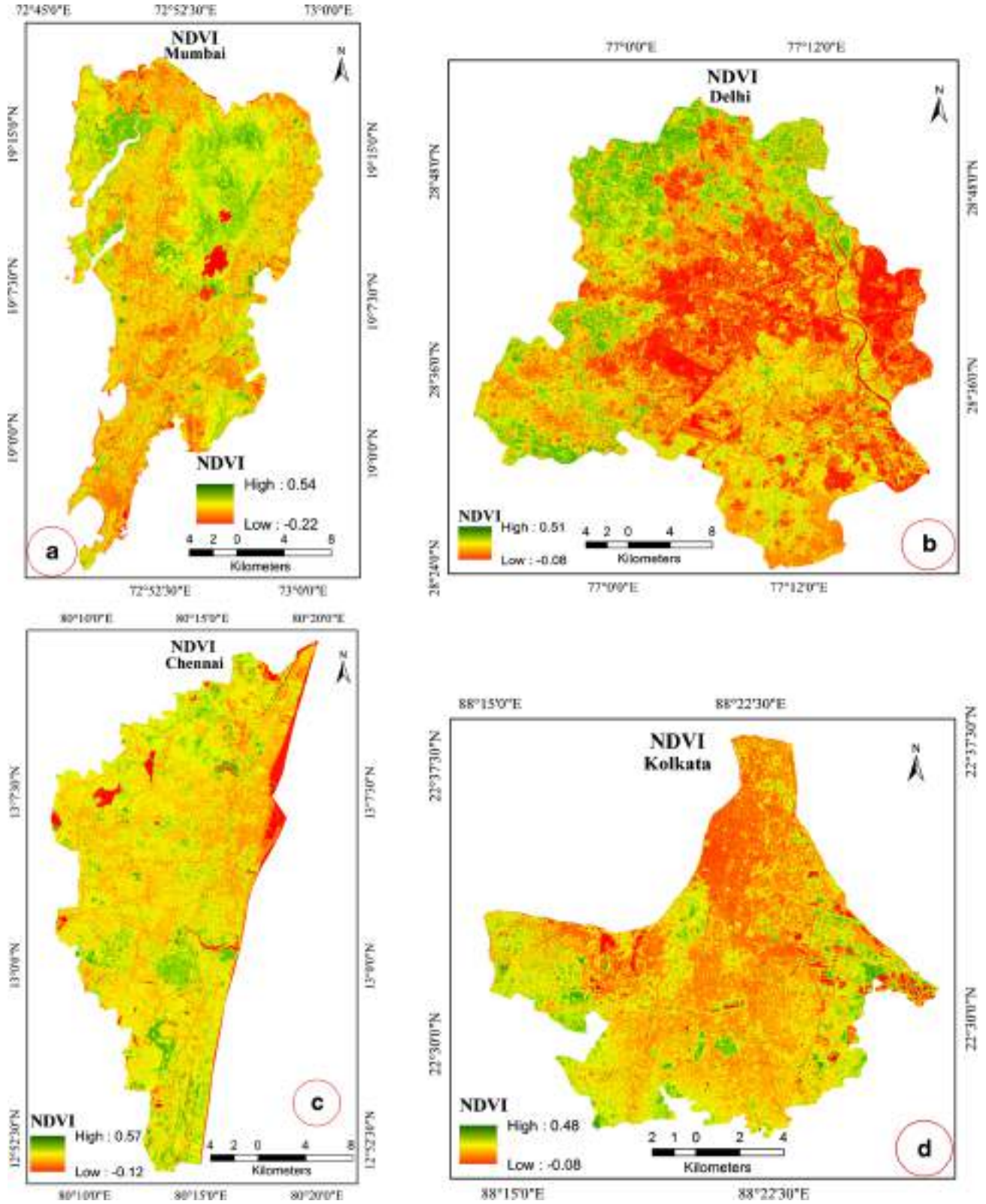

Fig. 2 NDVI of **a** Mumbai, **b** Delhi, **c** Chennai, and **d** Kolkata

bay. The NDBI value was the lowest above the bays of the western part of the city as well as in small patches in the central and eastern parts (Fig. 3a). In Delhi, the NDVI value ranges between − 0.08 and 0.51 with highest values in the northern and western parts. The central, south, and east Delhi have the lowest NDVI values, especially the Old

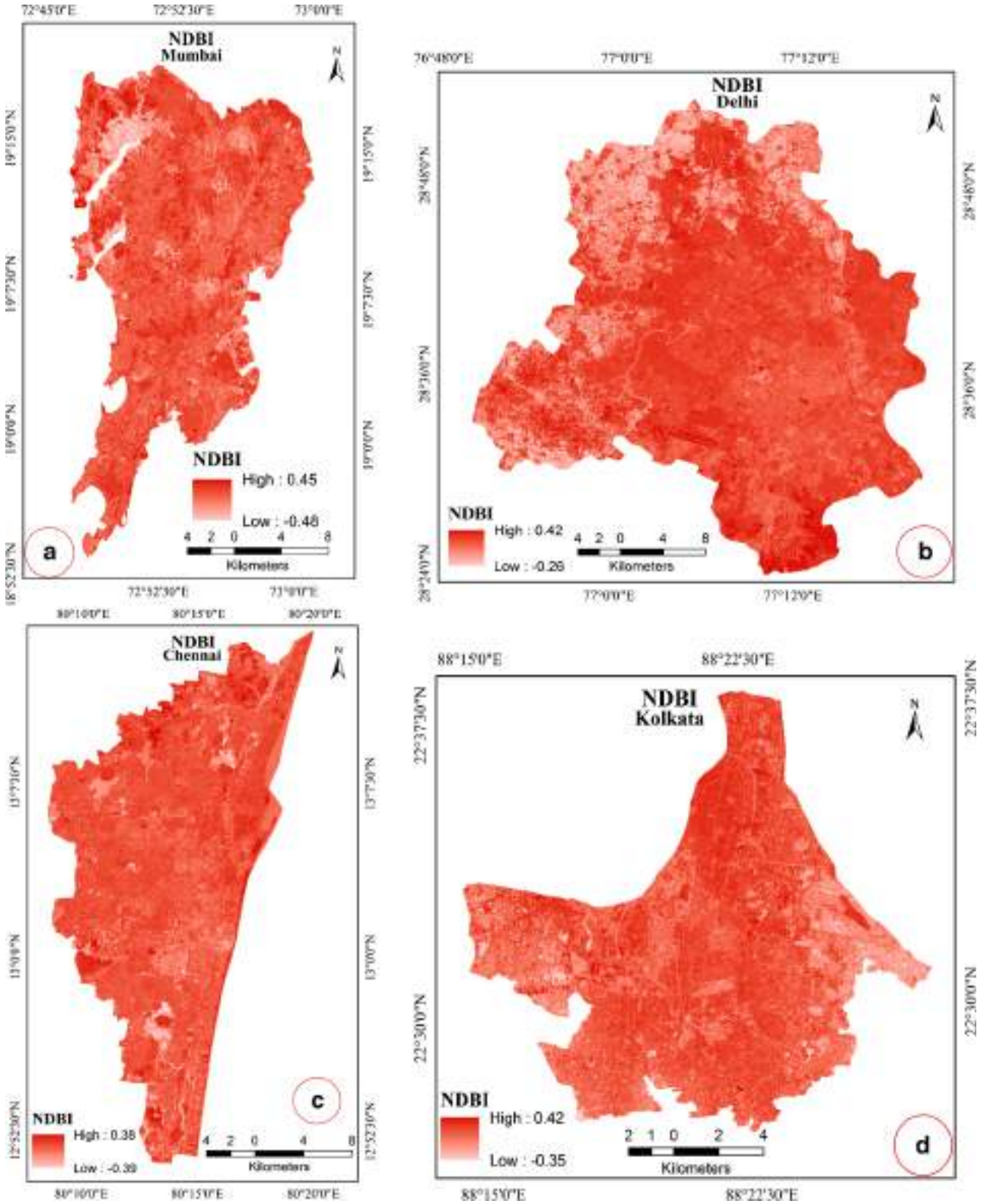

Fig. 3 NDBI of **a** Mumbai, **b** Delhi, **c** Chennai, and **d** Kolkata

Delhi region because of the presence of dense built-up surfaces and high-rise buildings, while the NDVI value is moderate to high along the Yamuna River, adjacent to East Delhi, as this part has forest cover as well as agricultural lands (Fig. 2b). Contrary to NDVI, the NDBI value of Delhi ranges between − 0.26 and 0.42, with highest values in southern Delhi.

Central and eastern Delhi also have high NDBI values, while the NDBI is low in a belt from north to south in western Delhi (Fig. 3b).

The NDVI and NDBI values of Chennai range between − 0.12 and 0.57 and − 0.39 and 0.38 respectively. The NDVI was low in most parts of the city, and high NDVI was concentrated in small patches in all parts of the city. The NDVI was maximum in the north-west and southern parts of the city, while a large patch of high NDVI can be seen in the central part below the bay area (Fig. 2c). A large belt of low NDVI can be seen along the eastern seacoast, while the NDVI value is also low in the north-west. Contrary to this, the NDBI value was comparatively high in all parts of the city and was maximum in the north and south as well as in the western extremes of the city. The patches of low NDBI were concentrated in the southern parts especially over Puzhal Lake and Cholavaram Tank as well as in the northern Chennai (Fig. 3c). Among all the cities, Kolkata has the least NDVI value, while the NDBI was also quite low. The NDVI value was high in eastern parts around wetlands (in Salt lakes region) and in the south-west of the city, and small patches of high NDVI occur in the north-western parts (Fig. 2d). The central and northern parts have the least NDVI values. On the other hand, the NDBI value was the highest in the northern parts (around Dum-Dum Airport) of the city, while central Kolkata also has a high NDBI. The NDBI was the least in the eastern as well as western part and on the northern extreme of the city (Fig. 3d).

Analysis of land surface temperature

Analysis of statistical values of LST-MWA and SWA

The descriptive statistics of urban land surface temperature (ULST) retrieved using both MWA and SWA shows that the highest of both minimum and maximum LST was in Mumbai followed by Chennai and Delhi, while Kolkata has the least LST, while the mean LST was the highest in Chennai, while Mumbai stands second in mean LST in both methods (Table 8). The standard deviation of LST was the highest in Mumbai followed by Chennai and Delhi, while Kolkata has the least standard deviation of LST, which describes that the former two cities have maximum variation in LST and the latter have the least variation.

While discussing the difference between descriptive statistics of LST, there exists a varying difference between the minimum, maximum, mean, and the standard deviation in LST for all the cities in both the MWA and SWA methods. The pattern of difference was the same in all statistical measures, i.e., maximum, minimum, mean, and standard deviation. Mumbai has the maximum difference followed by Chennai and Kolkata, while Delhi has the least difference between statistical measures of MWA and SWA land surface temperature. This is because the atmospheric effects (effect of atmospheric water vapor content) are higher over Mumbai and Chennai due to their proximity with the sea than Kolkata, while Delhi is a continental city located far away from the seas, thus it has the least atmospheric effects. Also, the comparison from in situ LST shows that the LST gape was lower for the SWA than the MWA in Mumbai and Chennai, and the coefficient of correlation (0.84 for Mumbai and 0.83 for Chennai) was higher than those of Delhi and Kolkata. At the same time, the LST gape was lower between in situ LST and LST retrieved using the MWA in Delhi and Kolkata, and the correlation coefficient was higher between the MWA and in situ LST than Mumbai and Chennai (Table 6).

Analysis of spatial pattern of LST

Although there are differences between descriptive statistics of MWA and SWA methods of the LST for all cities, the spatial pattern of LST retrieved using both methods was similar. The highest LST was found in Mumbai, ranging between 25.41 and 44.41 in MWA (Fig. 4a) and 28.81 and 56.62 in SWA (Fig. 4b), but the distribution of LST was highly uneven. A belt of very high LST was dispersed from the north to south of the city, and the highest LST is found in the central Mumbai near the CST Airport. The LST was low in the northern parts adjacent to the bay area and in a belt from the central part above the Virar and Tulsi Lakes to up to the northern extreme of the city (Fig. 4a & b). The patches of low LST were concentrated all over Mumbai city. In Delhi, the spatial pattern of LST was clearer than that of Mumbai and varies between 21.94 and 39.08 for MWA (Fig. 4c) and 25.04 and 47.21 for SWA (Fig. 4d). The high LST was found in patches located in the south, west, and northern parts especially in Old Delhi and in South Delhi, while the LST was low in the north of the city from east to west, and in south-western of the city, a belt of low LST from north to south can be seen over Yamuna River adjacent to East Delhi. The patches of high LST can be found in east Delhi also because this part of Delhi has very highly dense built-up surfaces.

The spatial pattern of LST in Chennai was less uneven in comparison with that of Delhi and Kolkata, and the LST varies between 26.46 and 43.56 in MWA (Fig. 5a) and 28.80 and 55.36 in SWA (Fig. 5b). The LST was very high in the northern parts as well as in the west-central part of the city, especially around the airport. The patches of high LST were distributed in the southern part of the city, while the LST was low in east, extreme north, and southern parts of the city. The patches of low LST were distributed all over the city especially at the outskirts of the city. Among all cities, Kolkata has the least minimum and maximum LST in both methods, and it ranges between 24.46 and 35.86 in MWA (Fig. 5c) and 27.13 and 44.27 in SWA (Fig. 5d). The pattern of distribution was very clear, and the LST is very high in the north especially in old parts of the city as well as in the west-

Table 8 Descriptive statistics of LST-MWA and LST-SWA for all cities

Cities	LST mono-window (°C)				LST split-window (°C)				Difference between split- and mono-window LST (°C)			
	Min.	Max.	Mean	SD	Min.	Max.	Mean	SD	Min.	Max.	Mean	SD
Mumbai	25.41	44.41	33.48	2.67	28.81	56.62	39.76	3.78	3.40	12.21	6.26	1.11
Delhi	21.94	39.01	29.42	2.05	25.04	47.21	34.19	2.45	3.10	8.20	4.77	0.40
Chennai	26.46	43.56	35.18	2.08	28.80	55.25	40.79	2.90	2.34	11.69	5.61	0.82
Kolkata	24.46	35.85	29.33	1.54	27.13	44.27	34.17	2.18	2.67	8.42	4.84	0.64

Min., minimum; *Max.*, maximum; *SD*, standard deviation

central parts, while the western and eastern parts have very low LST in Kolkata.

Analysis of relationships between NDVI, NDBI, and LST

To know the relationships between LU/LC type and LST, Weng (2001) tried to link the LU/LC with thermal signatures. Thus, sample points of land use indices and LST imageries were used for the investigation of their spatial relationships. The regression analysis shows moderate to high relationships between the NDBI, NDVI, and LST for all the cities. The scatter plots show an increasing trend of LST with increasing NDBI values (Fig. 6) while a decreasing trend in LST with increasing NDVI (Fig. 7). Among all the cities, Chennai has the highest regression coefficient between LST and NDBI, while Kolkata has the least on the other hand between LST and NDVI, Delhi has the highest, and Kolkata has the least regression coefficient (Table 9). The regression coefficients of LST and NDBI which was shown by r^2 value for the Mumbai, Delhi, Chennai, and Kolkata were 0.5077, 0.2344, 0.5484, and 0.4542 respectively, while the r^2 values of LST and NDVI for Mumbai, Delhi, Chennai, and Kolkata were 0.4433, 0.4863, 0.4787, and 0.4154 respectively.

The coefficient of determination (multiple r^2 in the regression table) varies between 0 and 1 (both positive and negative), with no correlation at 0 and perfect correlation at 1. The correlation value between 0.01 and 0.25 shows a weak correlation, between 0.26 and 0.50 moderate correlation, and above 0.51 high correlations. Generally, the correlation value above 0.9 is considered the perfect correlation. The multiple r^2 (coefficient of determination) shows the high correlation of NDBI and NDVI with LST for all the cities (Table 9), although in Fig. 6, the upswing in trend line shows that the correlation is positive between NDBI and LST, while in Fig. 7, the downswing in trend line shows that the correlation is negative between NDVI and LST for all the cities, which means that the higher the built-up surface, the higher will be the LST, and the lower the built-up surface, the lower will be the LST, while the situation will be negative in the case of vegetation as vegetation has a negative correlation with LST. Among all the cities, the coefficient of determination was the least in the case of Kolkata for both NDBI and NDVI, while it was the highest in Chennai for NDBI and in Delhi for NDVI (Table 9), which means that the built-up area has the highest impact on LST in Chennai while vegetation has the highest impact in Delhi.

Discussion

The present study deals with the surface heating pattern and its relationship with the built and vegetated surfaces in the selected Indian cities. This study was carried out because the rapid urbanization has led to a significant impact on the thermal environment of the cities (McCarthy et al. 2010). The built-up surfaces (NDBI) is the most important determinant of LST as it increases the temperature due to its thermodynamics and heat-observing capacity, while vegetated surfaces (NDVI) reduce the temperature because it reflects the temperature in the process of evapotranspiration (Khandelwal et al. 2018). It can be seen that the NDBI has a direct positive relationship with LST, while NDVI has a negative relationship with LST, as in the case of other studies like Ibrahim (2017) and Weng (2001).

In this study, two algorithms, i.e., MWA and SWA, were applied to analyze the LST pattern over the cities to see the difference between the LST retrieved from these two algorithms and to suggest which algorithms suit most in which type of climate. LST extracted using these two methods has a difference of about 4 °C (in the case of minimum LST) in Kolkata but more than 12 °C (in the case of maximum LST) in Chennai and Mumbai. The accuracy of emissivity estimation plays a vital role in the retrieval of LST, especially for urban areas (Chen et al. 2016). These ground-based measurements of the surface emissivity were taken from each city. The coefficient of correlation shows strong and positive relationships between the estimated and in situ emissivity for all cities (Table 6). A few studies have found the SWA to be a more accurate algorithm for the LST retrieval (Jiménez-Muñoz et al. 2014; Becker and Li 1990); at the same time, other studies found the MWA to be more accurate (Qin et al.

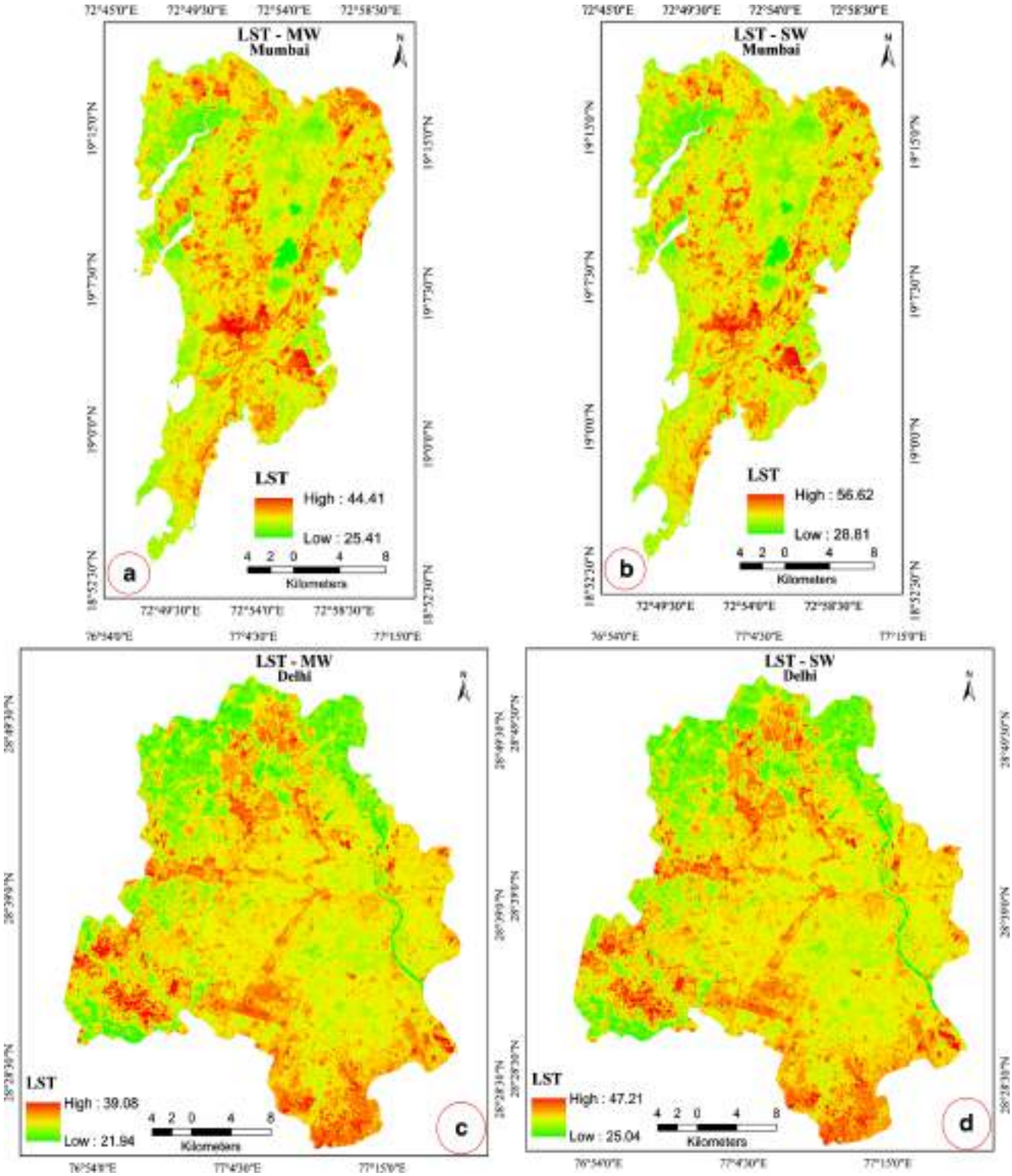

Fig. 4 LST mono-window of **a** Mumbai and **c** Delhi and LST split-window of **b** Mumbai and **d** Delhi

2001). The result shows a higher difference between the in situ LST and satellite LST in the SWA than the MWA for all the cities except Delhi, where the condition is reversed. Thus, MWA is found to be more accurate for the inland city, while the SWA is found to be more accurate for the maritime cities.

The spatial pattern of NDBI and NDVI of an area determines the spatial pattern of LST (Guha and Govil 2020; Guha et al. 2018). The histogram of NDBI and NDVI shows that Delhi has the maximum area under positive NDBI and NDVI followed by Mumbai and Chennai (Fig. 8), while Kolkata

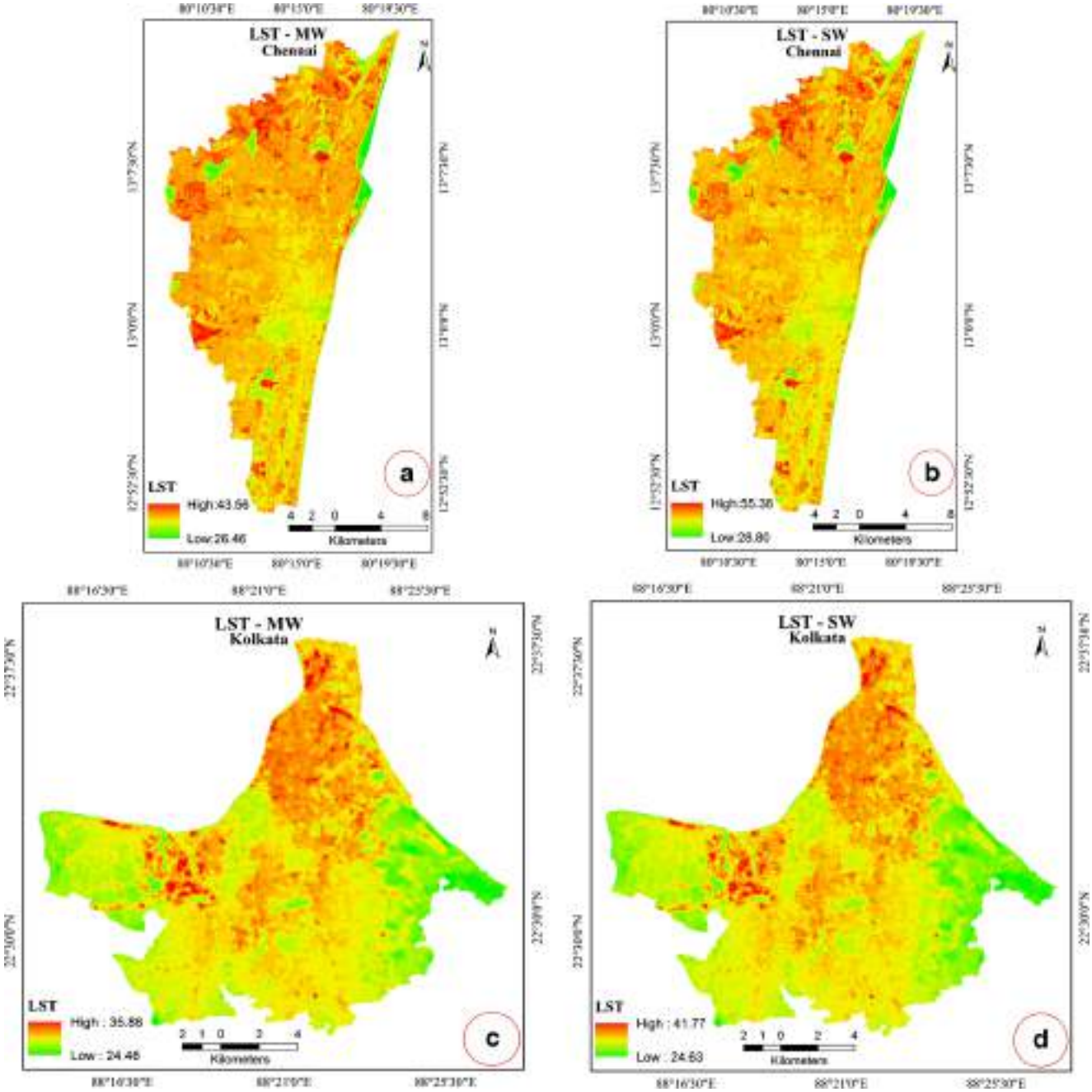

Fig. 5 LST mono-window of **a** Chennai and **c** Kolkata and split-window of **b** Chennai and **d** Kolkata

has the least. On the other hand, the histogram of LST shows that maximum pixels with higher LST (> 30 °C) were in Chennai followed by Mumbai and Delhi, while Kolkata has the least pixels above 30 °C (Fig. 8).

Usually, the climatic conditions change with latitude, but in India, the climatic elements (temperature, precipitation, humidity, etc.) vary in both east-west (longitudinal) and north-south (latitudinal) directions (Das and Hunt 2007). Furthermore, the literature survey from the previous studies suggests that there has been a variation of LST in cities located on different longitudes (Aithal et al. 2019; Ghosh et al. 2019; Sahana et al. 2019; Grover and Singh 2015). Among all the cities, Mumbai has the highest LST, followed by Chennai and Delhi, while Kolkata shows the lowest LST among all the cities (Table 7). This shows that the LST decreases with decreasing longitude, as Mumbai which is located on the highest longitude has the highest LST among all cities followed by Chennai and Delhi, while Kolkata which is on the lowest longitude among all cities has the least LST (Table 1). The spatial pattern of LST shows that the belt of high LST in

Table 9 Statistics from regression analysis of LST with NDBI and NDVI

S. No.	Cities	No. of observation	Regression between NDBI and LST				Regression between NDVI and LST			
			r^2	Adjusted r^2	Standard error	Multiple R	r^2	Adjusted r^2	Standard error	Multiple R
1	Mumbai	300	0.5077	0.5060	3.27	0.7125	0.4433	0.4414	3.48	0.6658
2	Delhi	600	0.2344	0.2324	3.56	0.4831	0.4862	0.4852	2.91	0.6972
3	Chennai	250	0.5484	0.5466	3.61	0.7405	0.4787	0.4766	3.88	0.6919
4	Kolkata	200	0.4542	0.4514	2.07	0.6739	0.4154	0.4124	2.14	0.6415

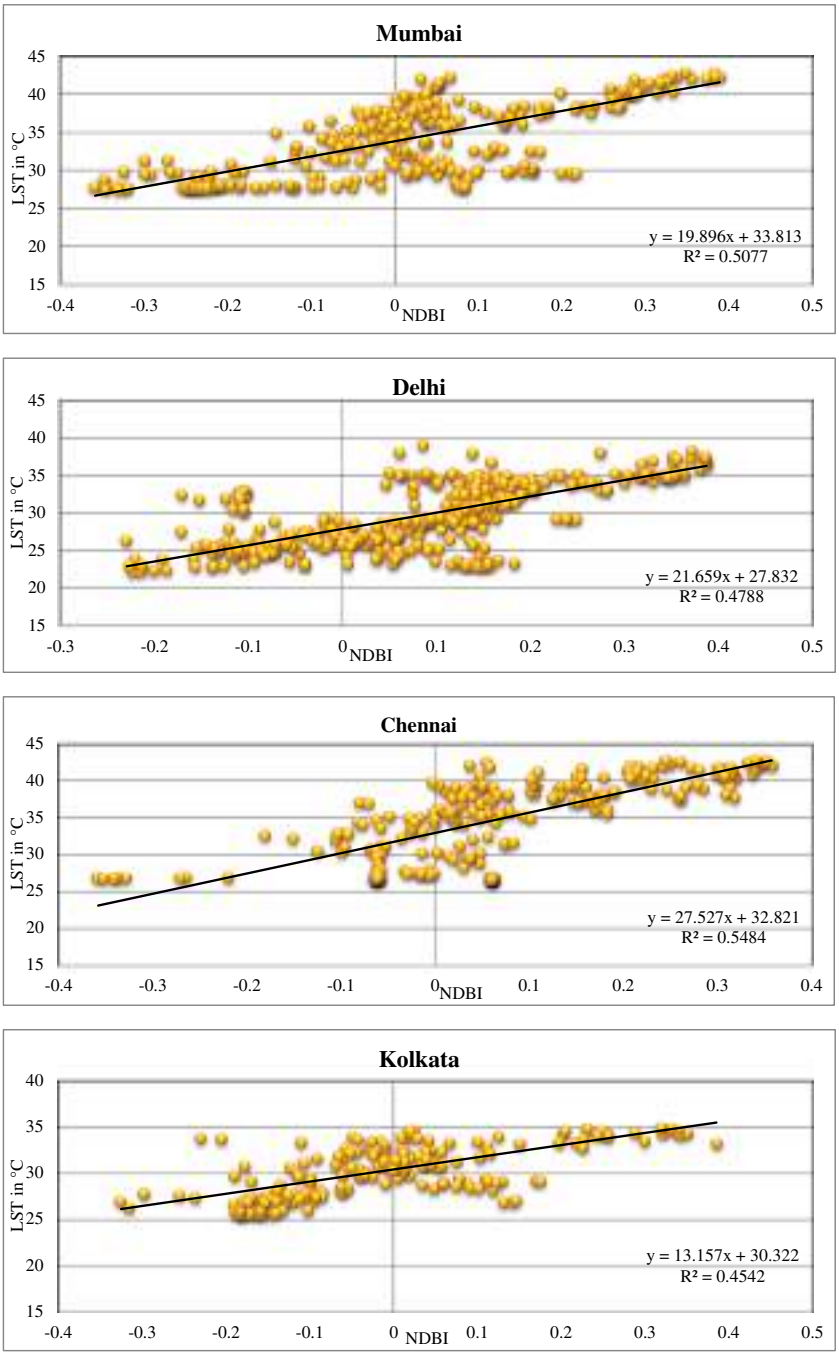

Fig. 6 Regression line and scatter plots of NDBI and LST for all cities

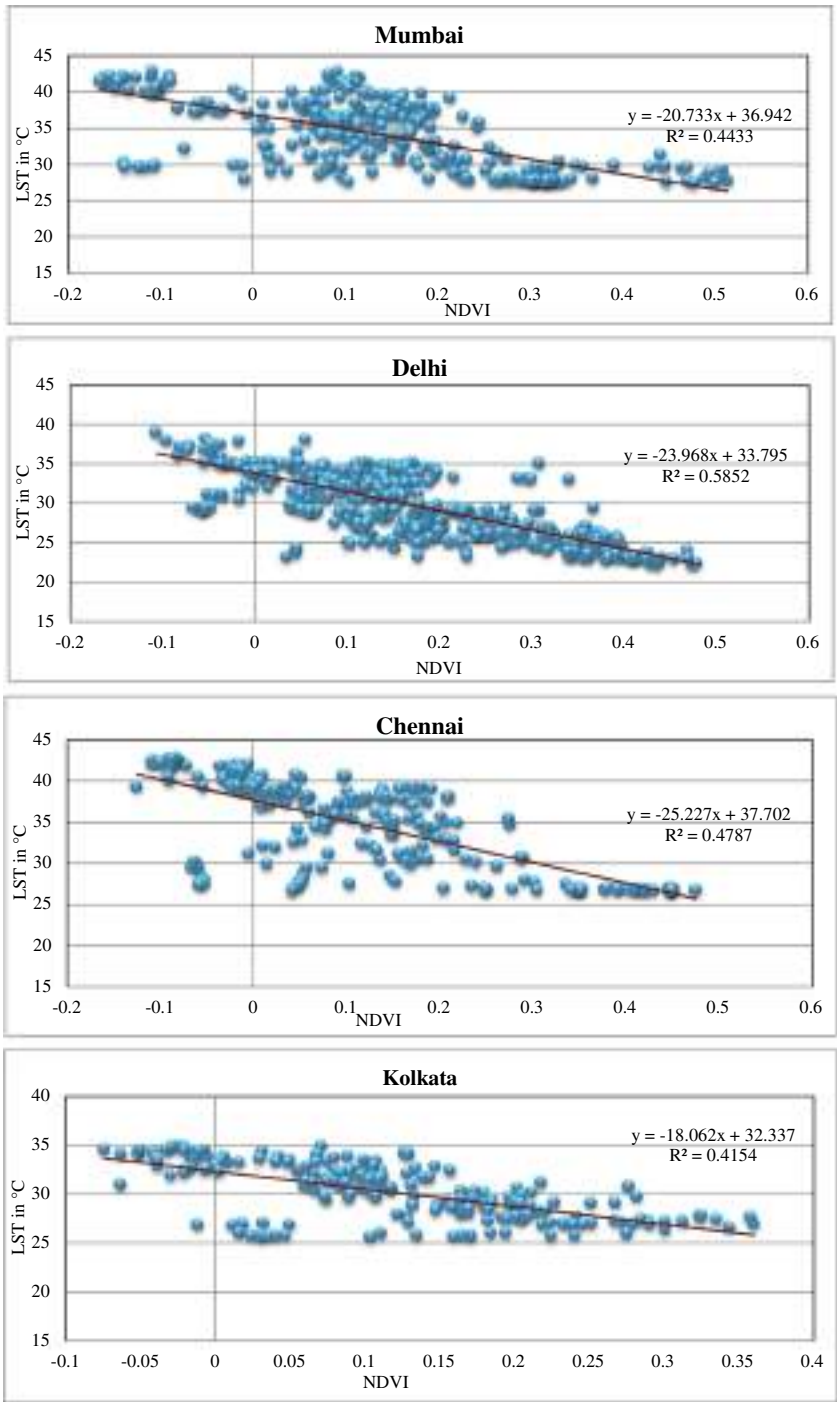

Fig. 7 Regression line and scatter plot of NDVI and LST for all cities

Mumbai and Kolkata is concentrated mostly in the central parts, while in Delhi and Chennai, it is concentrated in outskirts of the city.

The distribution of LST is controlled by different surface and climatic elements in different parts of the globe like land use pattern, altitude, latitude, and population density (Khandelwal et al. 2018; Mallick and Rahman 2012). The result shows that the effect of NDVI and NDBI was not the same in all cities, as the value of the varying r^2 shows the variation in the regression coefficient. The ULST varies from cities to cities and with time, as one city has a different pattern of LST than the others (Aithal et al. 2019; Bonafoni and Keeratikasikorn 2018). Each city has a distinctive climatic system which makes it different from the others. Kolkata is located in the eastern part of India, and this part of India experiences anti-cyclonic thundershower during March and April (pre-monsoon months), known as Norwesters, originating due to pressure differences over the land surface and in the

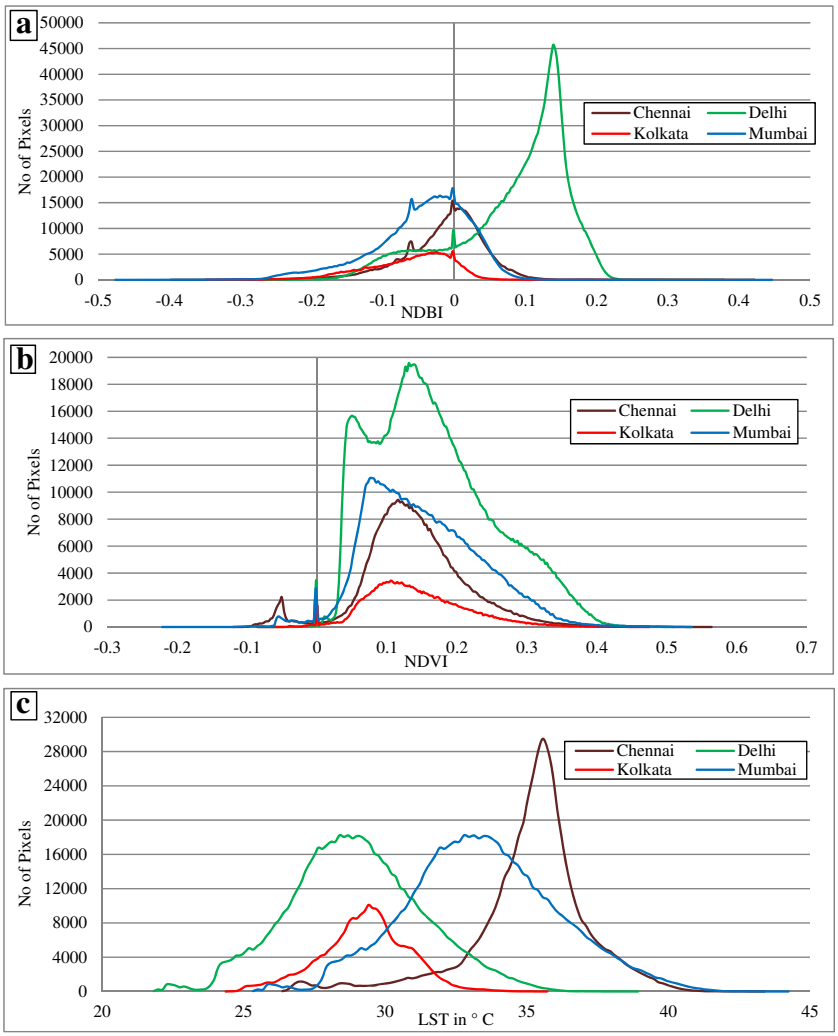

Fig. 8 Histogram for **a** NDBI, **b** NDVI, and **c** LST for all the cities

bay of Bengal (TOI 2018; Sadhukhan et al. 2000), which increases the soil moisture and enhances the vegetation growth. Thus, the LST is the lowest in Kolkata as soil moisture and vegetation have a negative impact on LST (Zhang et al. 2015). Delhi is a continental city having low variation in temperature and other climatic elements, thus it has a moderate LST. Chennai and Mumbai are maritime cities having very less climatic variations and have higher average air temperature than other cities, thus they have higher LST compared with Delhi and Kolkata.

The spatial relationship between NDBI and LST shows a positive relationship for all the cities. The densities of built surface and vegetation cover are important determinants of LST in urban areas, as the higher density of built surface raises the LST (Pramanik and Punia 2019), while a high density of vegetation cover significantly reduces the LST (Mwangi et al. 2018; Ogashawara and Bastos 2012). The coefficient of determination between LST and NDBI was moderate in the case of Delhi and Kolkata, while strong in the case of Mumbai and Chennai. Chennai has the highest coefficient of determination between LST and NDBI (0.54), while Kolkata has a comparatively low degree of correlation among all the cities, which means that in Kolkata, the impact of the built-up surface is less on LST among all the cities. The coefficient of determination between LST and NDVI shows a negative and moderate to high degree of correlation for all cities, and the degree of correlation was the highest for Delhi (0.58) followed by Kolkata and Mumbai, while Chennai has the least correlation between LST and NDVI among all the selected cities. Previous studies found that water bodies and moisture content have more effect on LST in maritime cities (Sahana et al. 2019; Grover and Singh 2015), while vegetation cover is the most important factor influencing LST in inland cities (Aithal et al. 2019). Thus, this study found that LST is more influenced by vegetation covers in inland areas than in maritime areas, while in maritime areas, the LST is more influenced by built-up surfaces.

Conclusion

The Landsat 8 (OLI/TIRS) data of March 2017 is used to assess the spatial pattern of LST and its relationships with NDVI and

NDBI for the four largest metro cities of India selected from different longitudes. Two different algorithms of LST retrieval were applied to assess the LST difference between the algorithms in the different climatic conditions. The study shows that the LST is comparatively higher in Chennai and Mumbai than Kolkata and Delhi although the vegetation cover is more pronounced in Mumbai and Chennai than Kolkata and Delhi. Furthermore, it is seen that the NDBI is more effective in the study of LST than NDVI in any climatic condition and in any part of the world because NDVI depends on and varies with climatic conditions while the NDBI is not dependent on climate, thus it remains the same throughout the year and in any climatic conditions. The study shows that the LST is found to be the lowest in Kolkata, which means that LST is getting more controlled by other factors in Kolkata than built-up surfaces and vegetation covers.

The linear regression analysis was applied to analyze the spatial relationship of LST with NDBI and NDVI for selected pixels, which shows that both built-up surface and vegetation cover have a different degree of correlation with LST. In Mumbai and Chennai, the built-up surface has a higher coefficient of determination with LST, while in Delhi and Kolkata, the vegetation cover has higher impacts on LST. Thus, this study concludes that in maritime cities, the built-up surfaces have more impact on the LST than inland cities, and in inland cities, the vegetation cover has a higher impact on LST than in maritime cities. It is suggested for future research that LST can be retrieved at different spatial resolutions and for different seasons of the year to assess the LST where some other factors such as soil moisture, water bodies, and population density can be applied to assess their impact on LST in these cities.

Acknowledgments The authors are thankful to the Survey of India for providing the Toposheet from which the city maps were obtained and the USGS Earth Explorer server (https://earthexplorer.usgs.gov/) for providing the satellite data. The authors are also thankful to Mr Azhar Nawaz of the Department of English, Aligarh Muslim University, Aligarh, India, for helping in improving English and the grammatical errors from the manuscript. The authors are highly thankful to the learned reviewer for their scholarly comments which lead to significant improvement of the MS.

Funding The lead author is thankful to the University Grant Commission (UGC) for providing the Junior Research Fellowship (JRF) for the doctoral research.

Compliance with ethical standards

Conflict of interest The authors declare that they have no conflict of interest.

References

Aithal BH, Chandan MC, Nimish G (2019) Assessing land surface temperature and land use change through spatio-temporal analysis: a case study of select major cities of India. Arab J Geosci 12:3. https://doi.org/10.1007/s12517-019-4547-1

Aldhshan SRS, Shafri HZM (2019) Change detection on land use/land cover and land surface temperature using spatiotemporal data of Landsat: a case study of Gaza Strip. Arab J Geosci 12:443. https://doi.org/10.1007/s12517-019-4597-4

Amirtham LR, Devdas MD, Perumal M (2009) Mapping of micro-urban heat islands and land cover changes: a case in Chennai City, India. Int J Clim Chang: Impacts Response 1:71–84. https://doi.org/10.18848/1835-7156/CGP/v01i02/37258

Artis DA, Carnahan WH (1982) Survey of emissivity variability in thermography of urban areas. Remote Sens Environ 12:313–329. https://doi.org/10.1016/0034-4257(82)90043-8

Asgarian A, Amiri BJ, Sakieh Y (2014) Assessing the effect of green cover spatial patterns on urban land surface temperature using landscape metrics approach. Urban Ecosyst 18:209–222. https://doi.org/10.1007/s11252-014-0387-7

Becker F, Li ZL (1990) Towards a local split window method over land surfaces. Int J Remote Sens 11(3):369–393. https://doi.org/10.1080/01431169008955028

Bian T, Ren G, Yue Y (2017) Effect of urbanization on land-surface temperature at an urban climate station in North China. Bound-Layer Meteorol 165:553–567. https://doi.org/10.1007/s10546-017-0282-x

Bonafoni S, Keeratikasikorn C (2018) Land surface temperature and urban density: multiyear modeling and relationship analysis using MODIS and Landsat data. Remote Sens 10(9):1471. https://doi.org/10.3390/rs10091471

Carlson TN, Ripley DA (1997) On the relation between NDVI, fractional vegetation cover, and leaf area index. Remote Sens Environ 62(3):241–252

Census of India (2011) City census. https://www.census2011.co.in/city.php (Accessed Oct 2019).

Chander G, Markhan BL, Helder DL (2009) Summary of current radiometric calibration coefficients for Landsat MSS, TM, ETM+, and EO-1 ALI sensors. Remote Sens Environ 113:893–903

Chen X, Zhao H, Li P, Yin Z (2006) Remote sensing image-based analysis of the relationship between urban heat island and land use/cover changes. Remote Sens Environ 104(2):133–146

Chen F, Song Y, Su Z, Wang K (2016) Effect of emissivity uncertainty on surface temperature retrieval over urban areas: investigations based on spectral libraries. ISPRS J Photogramm Remote Sens 114:53–65

Chettry V, Surawar M (2020) Urban sprawl assessment in Raipur and Bhubaneswar urban agglomerations from 1991 to 2018 using geoinformatics. Arab J Geosci 13:667. https://doi.org/10.1007/s12517-020-05693-0

Connors JP, Galletti CS, Chow WTL (2013) Landscape configuration and urban heat island effects: assessing the relationship between landscape characteristics and land surface temperature in Phoenix, Arizona. Landsc Ecol 28:271–283. https://doi.org/10.1007/s10980-012-9833-1

Das SK, Hunt JCR (2007) Variability of climate change in India. Curr Sci 93(6):782–788

Deng Y, Wang S, Bai X, Tian Y, Wu L, Xiao J, Chen F, Qian Q (2017) Relationship among land surface temperature and LUCC, NDVI in typical Karst area. Sci Rep 8(1):641

Dhorde A, Dhorde A, Gadgil AS (2009) Long-term temperature trends at four largest cities of India during the twentieth century. J Ind Geophys Union 13(2):85–97

Dutta D, Rahman A, Paul SK, Kundu A (2019) Changing pattern of urban landscape and its effect on land surface temperature in and around Delhi. Environ Monit Assess 191:551. https://doi.org/10.1007/s10661-019-7645-3

Dwivedi A, Khire MV (2018) Application of split-window algorithm to study urban heat island effect in Mumbai through land surface

temperature approach. Sustain Cities Soc 41:865–877. https://doi.org/10.1016/j.scs.2018.02.030

Fan C, Myint SW, Kaplan S, Middel A, Zheng B, Rahman A, Huang HP, Brazel A, Blumberg DG (2017) Understanding the impact of urbanization on surface urban heat islands—a longitudinal analysis of the oasis effect in subtropical desert cities. Remote Sens 9(7):672. https://doi.org/10.3390/rs9070672

Franca GB, Cracknell AP (1994) Retrieval of land and sea surface temperature using NOAA-11 AVHRR data in north-eastern Brazil. Int J Remote Sens 15:1695–1712. https://doi.org/10.1080/01431169408954201

Fu P, Weng Q (2018) Variability in annual temperature cycle in the urban areas of the United States as revealed by MODIS imagery. ISPRS J Photogramm Remote Sens 146:65–73. https://doi.org/10.1016/j.isprsjprs.2018.09.003

Ghosh S, Chaterjee ND, Dinda S (2019) Relation between urban biophysical composition and dynamics of land surface temperature in the Kolkata metropolitan area: a GIS and statistical based analysis for sustainable planning. Model Earth Syst Environ 5:307–329. https://doi.org/10.1007/s40808-018-0535-9

Grover A, Singh RB (2015) Analysis of urban heat island (UHI) in relation to normalized difference vegetation index (NDVI): a comparative study of Delhi and Mumbai. Environments 2:125–138

Guha S, Govil H (2020) An assessment on the relationship between land surface temperature and normalized difference vegetation index. Environ Dev Sustain. https://doi.org/10.1007/s10668-020-00657-6

Guha S, Govil H, Dey A, Gill N (2018) Analytical study of land surface temperature with NDVI and NDBI using Landsat 8 OLI and TIRS data in Florence and Naples city, Italy. Eur J Remote Sens 51(1):667–678. https://doi.org/10.1080/22797254.2018.1474494

Guo Z, Wang SD, Cheng MM, Shu Y (2012) Assess the effect of different degrees of urbanization on land surface temperature using remote sensing images. Procedia Environ Sci 13:935–942. https://doi.org/10.1016/j.proenv.2012.01.087

Ibrahim GRF (2017) Urban land use land cover changes and their effect on land surface temperature: case study using Dohuk City in the Kurdistan region of Iraq. Climate 5(1):13. https://doi.org/10.3390/cli5010013

Jiménez-Muñoz JC, Sobrino JA, Skoković D, Mattar C, Cristóbal J (2014) Land surface temperature retrieval methods from Landsat-8 thermal infrared sensor data. IEEE Geosci Remote Sens Lett 11(10):1840–1843

Khadim N, Mourshe M, Bray M (2016) Advances in remote sensing applications for urban sustainability. Euro-Mediterr J Environ Integr 1:7. https://doi.org/10.1007/s41207-016-0007-4

Khandelwal S, Goyal R, Kaul N, Mathew A (2018) Assessment of land surface temperature variation due to change in elevation of area surrounding Jaipur, India. Egypt J Remote Sens Space Sci 21(1):87–94. https://doi.org/10.1016/j.ejrs.2017.01.005

Kumari B, Tayyab M, Shahfahad S, Mallick J, Khan MF, Rahman A (2018) Satellite-driven land surface temperature (LST) using Landsat 5, 7 (TM/ETM+ SLC) and Landsat 8 (OLI/TIRS) data and its association with built-up and green cover over urban Delhi. India. Remote Sens Earth Syst Sci 1:63–78. https://doi.org/10.1007/s41976-018-0004-2

Li ZL, Tang BH, Wu H, Ren H, Yan G, Wan Z, Trigo IF, Sobrino JA (2013) Satellite-derived land surface temperature: current status and perspectives. Remote Sens Environ 131:14–37. https://doi.org/10.1016/j.rse.2012.12.008

Li H, Zhou Y, Li X, Meng L, Wang X, Wu S, Sodoudi S (2018) A new method to quantify surface urban heat island intensity. Sci Total Environ 624:262–272. https://doi.org/10.1016/j.scitotenv.2017.11.360

Li Y, Schubert S, Kropp JP, Rybski D (2020) On the influence of density and morphology on the urban heat island intensity. Nat Commun 11:2647. https://doi.org/10.1038/s41467-020-16461-9

Liu F, Zhang X, Murayama Y, Morimoto T (2020) Impacts of land cover/use on the urban thermal environment: a comparative study of 10 megacities in China. Remote Sens 12(2):307. https://doi.org/10.3390/rs12020307

Lo CP, Quattrochi DA, Luvall JC (1997) Application of high resolution thermal infrared remote sensing and GIS to assess the urban heat island effect. Int J Remote Sens 18(2):287–304. https://doi.org/10.1080/014311697219079

Lombardo MA (1985) Ilha de Calor Nas Metrópoles: O Exemplo de São Paulo (in Portuguese). Hucitec, São Paulo, Brazil, pp. 244.

Lu D, Song K, Zeng L, Liu D, Khan S, Zhang B, Wang Z, Jin C (2008) Estimating impervious surface for the urban area expansion: examples from Changchun, Northeast China. In: The international archives of the photogrammetry, remote sensing and spatial information sciences, 36(Part B8), pp 385–391

Malik MS, Shukla JP, Mishra S (2019) Relationship of LST, NDBI and NDVI using Landsat-8 data in Kandaihimmat Watershed, Hoshangabad, India. Indian J Geo Marine Sci 48:25–31

Mallick J, Rahman A (2012) Impact of population density on surface temperature and micro-climate of Delhi. Curr Sci 102(12):1708–1713

Mallick J, Rahman A, Singh CK (2013) Modeling urban heat islands in heterogeneous land surface and its correlation with impervious surface area by using night-time ASTER satellite data in highly urbanizing city, Delhi-India. Adv Space Res 52(4):639–655

Mandal J, Ghosh N, Mukhopadhyay A (2019) Urban growth dynamics and changing land-use land-cover of megacity Kolkata and its environs. J Indian Soc Remote Sens 47:1707–1725. https://doi.org/10.1007/s12524-019-01020-7

Masoudi M, Tan PY, Liew SC (2019) Multi-city comparison of the relationships between spatial pattern and cooling effect of urban green spaces in four major Asian cities. Ecol Indic 98:200–213

McCarthy MP, Best MJ, Betts RA (2010) Climate change in cities due to global warming and urban effects. Geophys Res Lett 37(9):L09705. https://doi.org/10.1029/2010GL042845

McMillin LM (1975) Estimation of sea surface temperatures from two infrared window measurements with different absorption. J Geophys Res 80:5113–5117. https://doi.org/10.1029/JC080i036p05113

Mohajerani A, Bakaric J, Jeffrey-Bailey T (2017) The urban heat island effect, its causes, and mitigation, with reference to the thermal properties of asphalt concrete. J Environ Manag 197:522–538. https://doi.org/10.1016/j.jenvman.2017.03.095

Mujabar S, Rao V (2018) Estimation and analysis of land surface temperature of Jubail industrial city, Saudi Arabia, by using remote sensing and GIS technologies. Arab J Geosci 11:742. https://doi.org/10.1007/s12517-018-4109-y

Munslow B, O'Dempsey T (2010) Globalisation and climate change in Asia: the urban health impact. Third World Q 31(8):1339–1356. https://doi.org/10.1080/01436597.2010.541082

Mwangi PW, Karanja FN, Kamau PK (2018) Analysis of the relationship between land surface temperature and vegetation and built-up indices in Upper-Hill, Nairobi. J Geosci Environ Prot 6:1–16. https://doi.org/10.4236/gep.2018.61001

Ogashawara I, Bastos V (2012) A quantitative approach for analyzing the relationship between urban heat islands and land cover. Remote Sens 4(11):3596

Omidvar H, Bou-Zeid E, Chiaramonte M (2019) Physical determinants and reduced models of the rapid cooling of urban surfaces during rainfall. J Adv Model Earth Syst 11:1364–1380. https://doi.org/10.1029/2018MS001528

Patra S, Sahoo S, Mishra P, Mahapatra SC (2018) Impacts of urbanization on land use/cover changes and its probable implications on local climate and groundwater level. J Urban Manag 7(2):70–84

Pramanik S, Punia M (2019) Land use/land cover change and surface urban heat island intensity: source–sink landscape-based study in

Delhi, India. Environ Dev Sustain. https://doi.org/10.1007/s10668-019-00515-0

Qin Z, Karnieli A, Berliner P (2001) A mono-window algorithm for retrieving land surface temperature from Landsat TM data and its application to the Israel-Egypt border region. Int J Remote Sens 22(18):3719–3746

Rahman A, Aggarwal SP, Netzband M, Fazal S (2011) Monitoring urban sprawl using remote sensing and GIS techniques of a fast growing urban centre, India. IEEE J Select Top Appl Earth Obs Remote Sens 4(1):56–64. https://doi.org/10.1109/jstars.2010.2084072

Rangoli G, Keshari AK, Gosain AK, Khosa R (2018) A mono-window algorithm for land surface temperature estimation from Landsat 8 thermal infrared sensor data: a case study of the Beas River Basin, India. Pertanika J Sci Technol 26(2):829–840

Sadhukhan I, Lohar D, Pal DK (2000) Pre-monsoon season rainfall variability over Gangetic West Bengal and its neighbourhood, India. Int J Climatol 20(12):1485–1493

Sahana M, Dutta S, Sajjad H (2019) Assessing land transformation and its relation with land surface temperature in Mumbai city, India using geospatial techniques. Int J Urban Sci 23(2):205–225. https://doi.org/10.1080/12265934.2018.1488604

Sekertekin A, Bonafoni S (2020) Land surface temperature retrieval from Landsat 5, 7, and 8 over rural areas: assessment of different retrieval algorithms and emissivity models and toolbox implementation. Remote Sens 12(2):294. https://doi.org/10.3390/rs12020294

Sharpe DM, Stearns F, Leitner LA, Dorney JR (1986) Fate of natural vegetation during urban development of rural landscapes in south eastern Wisconsin. Urban Ecol 3–4(9):267–287

Skokovic D, Sobrino JA, Jimenez-Muñoz JC, Soria G, Julien Y, Mattar C, Jordi C (2014) Calibration and validation of land surface temperature for LANDSAT8 TIRS sensor. Land product validation and evolution, ESA/ESRIN Frascati (Italy), pp 6–9

Sobrino JA, Jimenez-Munoz JC, Paolini L (2004) Land surface temperature retrieval from LANDSAT TM 5. Remote Sens Environ 90: 434–440

Su W, Gu C, Yang G (2010) Assessing the impact of land use/land cover on urban heat island pattern in Nanjing City, China. J Urban Plan Dev-ASCE 136(4):365–372

Sultana S, Satyanarayana ANV (2018) Urban heat island intensity during winter over metropolitan cities of India using remote-sensing techniques: impact of urbanization. Int J Remote Sens 39(20):6692–6730. https://doi.org/10.1080/01431161.2018.1466072

Takagi M, Gyokusen K (2004) Light and atmospheric pollution affect photosynthesis of street trees in urban environments. Urban For Urban Green 2:167–171

TOI (2018) Mercury may slide after a storm on Monday: Met Read more at: http://timesofindia.indiatimes.com/articleshow/63164175.cms?utm_source=contentofinterest&utm_medium=text&utm_campaign=cppstt (Accessed Nov 2019)

United Nations (2014) World population prospects (highlights), 2014 revision. Department of Economic and Social Affairs, New York. (Accessed Oct 2019)

Voogt JA, Oke TR (2003) Thermal remote sensing of urban climates. Remote Sens Environ 86:370–384. https://doi.org/10.1016/S0034-4257(03)00079-88

Wan Z, Dozier J (1996) A generalized split-window algorithm for retrieving land-surface temperature from space. IEEE Trans Geosci Remote Sens 34(4):892–905

Wang Y, Zhang Y, Ding N, Qin K, Yang X (2020) Simulating the impact of urban surface evapotranspiration on the urban heat island effect using the Modified RS-PM model: a case study of Xuzhou, China. Remote Sens 12(3):578. https://doi.org/10.3390/rs12030578

Weng Q (2001) A remote sensing-GIS evaluation of urban expansion and its impact on surface temperature in the Zhujiang Delta, China. Int J Remote Sens 22:1999–2014

Wonorahardjo S, Sutjahja IM, Mardiyati Y, Andoni H, Thomas D, Achsani RA, Steven S (2020) Characterising thermal behaviour of buildings and its effect on urban heat island in tropical areas. Int J Energy Environ Eng 11:129–142. https://doi.org/10.1007/s40095-019-00317-0

Xiao H, Weng Q (2007) The impact of land use and land cover changes on land surface temperature in a karst area of China. J Environ Manag 85:245–257. https://doi.org/10.1016/j.jenvman.2006.07.016

Xie Y, Sha Z, Yu M (2008) Remote sensing imagery in vegetation mapping: a review. J Plant Ecol 1(1):9–23. https://doi.org/10.1093/jpe/rtm005

Xue J, Su B (2017) Significant remote sensing vegetation indices: a review of developments and applications. J Sensors 2017:1–17. https://doi.org/10.1155/2017/1353691

Yang C, He X, Yan F, Yu L, Bu K, Yang J, Chang L, Zhang S (2017) Mapping the influence of land use/land cover changes on the urban heat island effect—a case study of Changchun. China. Sustainability 9(2):312. https://doi.org/10.3390/su90203122

Yu X, Guo X, Wu Z (2014) Land surface temperature retrieval from Landsat 8 TIRS—comparison between radiative transfer equation-based method, split window algorithm and single channel method. Remote Sens 6(10):9829–9852

Zha Y, Gao J, Ni S (2003) Use of normalized difference built-up index in automatically mapping urban areas from TM imagery. Int J Remote Sens 24:583–594. https://doi.org/10.1080/01431160304987

Zhang D, Tang R, Tang BH, Wu H, Li ZL (2015) A simple method for soil moisture determination from LST–VI feature space using non-linear interpolation based on thermal infrared remotely sensed data. IEEE J Sel Topics Appl Earth Observ Remote Sens 8(2):638–648

Zhang F, Tiyip T, Kung H, Johnson VC, Maimaitiyiming M, Zhou M, Wang J (2016) Dynamics of land surface temperature (LST) in response to land use and land cover (LULC) changes in the Weigan and Kuqa river oasis, Xinjiang, China. Arab J Geosci 9: 499. https://doi.org/10.1007/s12517-016-2521-8